J. Cent. South Univ. (2022) 29: 3544−3556
DOI: https://doi.org/10.1007/s11771-022-4968-y

Springer

Optimizing microstructure and mechanical properties of heat-treated Al-Zn-Mg-Cu alloy by indirect hot deformation technology

ZHANG Quan-da(张泉达)[1]*, SUN Fu-zhen(孙福臻)[1], LIU Meng(刘萌)[1, 2], LIU Wen-cai(刘文才)[3]

1. State Key Laboratory of Advanced Forming Technology and Equipment (China Academy of Machinery Science & Technology), Beijing 100044, China;
2. School of Mechanical Engineering, University of Science and Technology Beijing, Beijing 100083, China;
3. National Engineering Research Center of Light Alloy Net Forming and State Key Laboratory of Metal Matrix Composite (Shanghai Jiao Tong University), Shanghai 200240, China

Abstract: In this paper, the indirect thermal tensile experiments of 7075 aluminum alloy including the pre-deformation process at room temperature and the final heat tensile process were carried out, the plastic deformation behavior and forming limit of the material in the compound forming process were investigated considering three pre-deformation amounts 4%, 9%, 14%, two strain rates 0.001 s^{-1}, 0.01 s^{-1} and four forming temperatures 300 ℃, 350 ℃, 400 ℃, 450 ℃. In the indirect hot forming process, the material is sensitive to the pre-deformation, strain rate, and forming temperature, when the strain rate is 0.01 s^{-1}, the pre-deformation amount is 4%, and the forming temperature is 400 ℃, respectively, the maximum tensile deformation is 50 mm. Finally, taking the process in which the forming temperature is 450 ℃ as an example, according to the observation of the microstructure appearance of fracture, the fracture type in the hot forming process was judged as the ductile fracture. By analyzing the microstructure of the specimen treated with the quenching and artificial aging process, the eutectic T (AlZnMgCu) phase and α(Al) matrix formed a network of non-equilibrium alpha binary eutectic.

Key words: strain rate; pre-deformation; forming temperature; AA7075; compound tensile

Cite this article as: ZHANG Quan-da, SUN Fu-zhen, LIU Meng, LIU Wen-cai. Optimizing microstructure and mechanical properties of heat-treated Al-Zn-Mg-Cu alloy by indirect hot deformation technology [J]. Journal of Central South University, 2022, 29(11): 3544−3556. DOI: https://doi.org/10.1007/s11771-022-4968-y.

1 Introduction

With the progress of science and technology, the people's need for a better life is even stronger, so living environment has become the primary livelihood issue which needs to be solved by all countries. The exhaust gas emission of automobile industry is the main factor threatening environment protection. Therefore, all of the world have taken measures to reduce the exhaust emissions of automobile. Among them, the reduction of the car weight is an effective way. From the perspective of material science, the aluminum alloys have the advantage of low density compared with the steel, so, the application of aluminum alloy and other lightweight alloys in the automobile industry can greatly reduce the weight of the car. For the 6000

Foundation item: Project(SKL2020005) supported by the Open Fund of State Key Laboratory of Advanced Forming Technology and Equipment, China; Project(206Z1803G) supported by Local Science and Technology Development Fund Guided by the Central Government of China
Received date: 2021-02-02; **Accepted date:** 2021-08-17
Corresponding author: ZHANG Quan-da, PhD; Tel: +86-10-88301752; E-mail: zhangquandadgu@163.com; ORCID: https://orcid.org/0000-0003-4026-2999

and 5000 series aluminum alloys, they have high strength and light weight, so they are more widely used in the field of automobile industry at present.

At the same time, because the 7075 aluminum alloy belongs to the ultra-high-strength aluminum alloy, it has many advantages such as low density, high strength, high resistance to fatigue, strong impact resistance, and good corrosion resistance [1−6], all of these make it extensively used in the field of aerospace. Compared with 6000 and 5000 series aluminum alloys, its tensile strength can be up to 750 MPa after certain heat treatment [7], and it is of great practical significance to study the application considering the human safety and loss of weight. At the same time, the 7075 aluminum alloy has low elongation at room temperature which is caused by the gathering of dislocation pile-ups beside grain region boundaries [8−9], and is prone to cracking by traditional forming process, so the cold forming technology is rarely applied for the manufacturing process of 7000 series aluminum alloy [10 − 12]. Therefore, its application in the field of the automobile is limited.

Because the strength of the AA7075 can be improved after certain heat treatment, and its plastic flow property can be affected by the hot environment at the same time, some scholars currently have studied the forming technologies and establishment of the heat treatment system. XIAO [13] proposed a hot forming process of aluminum alloy, the plastic flow performance can be improved by utilizing the thermal circumstance in the hot forming process, which can effectively solve cracking problems. The 7075 aluminum alloy should be solution treated to form an unsaturated solid solution, then the strengthening phases precipitated by rapid quenching and artificial aging treatment, and its tensile strength increases eventually, so the solution treatment is needed before the forming process [14 − 16]. ZHANG et al [7] studied the heat treatment process of 7000 series aluminum alloys by using the orthogonal test. According to the heat treatment of 110 ℃, 4 h+ 150 ℃, 8 h, the tensile strength of the alloy can be up to 750.27 MPa, the yield strength can be up to 562.57 MPa, and the elongation was 26.43% finally. ROKNI et al [17] studied the deformation behaviors of 7075 aluminum alloy with different forming temperatures and deformation rates, and the results showed that the peak stress of the material was sensitive to strain rate and temperature.

The hot forming process of aluminum alloy contains solution treatment, forming, quick quenching and artificial aging, the plasticity of aluminum alloy can be improved, and the tensile strength can increase at the same time, so the hot forming technology of aluminum alloy is a research topic in the field of automotive lightweight recently. The hot forming process can be divided into direct hot forming and indirect hot forming. The direct hot forming technology is common, while, the indirect hot forming process includes pre-deformation, solution process, quenching and artificial treatment, and it was studied rarely. It is mainly for the special materials and parts with large deformation, which is very helpful to the weight reduction of the automobile industry. The key parameters such as pre-deformation ε_0 and forming temperature T in the solution process have a great influence on the forming limit and the strength after artificial treatment. Some researchers have also done their efforts to research the influence of parameters on the deformation process and strengthening mechanism. The strengthening mechanism of the 7075 aluminum alloy with ultra-fine grains after aging precipitation was quantitatively studied by MA et al [18 − 19]. WERT et al [20] studied the effect of grain size on the yield strength of 7000 series aluminum alloys, and confirmed the Hall-Petch relationship coefficient of 7075 aluminum alloys. At the same time, some materials are sensitive to the strain rate, and the deformation limit will be various under different deformation rates. For the deformation behavior of the alloy under the condition of high temperature, the influence effects of the forming temperature and strain rate on the plastic flow were investigated widely [21 − 22]. So, the research of the comprehensive effect of the pre-deformation, forming temperature and strain rate on the deformation limit and plastic flow property is greatly significative for the establishment of optimal indirect hot forming route, and it will be also helpful for the wide use of the high strength aluminum alloys in automobile lightweight manufacturing field. There are less reports about it.

2 Experimental

2.1 Experiment specimen and equipment

The experiment material is the aluminum alloy 7075 which is also called ultra-high-strength aluminum alloy, and the chemical compositions are shown in Table 1. Due to its excellent performances such as high strength and hardness, good corrosion resistance, and high toughness, it has become one of the most important structural materials [23]. The single tensile specimen was processed and tested according to the requirements of GB/T228.1—2015. The sizes of the specimen are shown in Figure 1.

Table 1 Chemical composition of 7075 aluminum alloy

wt%

Al	Si	Fe	Cu	Mn
Bal.	0.4	0.5	1.2−2.0	0.3
Mg	Zn	Ti	Cr	Other
2.1−2.9	5.1−6.1	0.2	0.18−0.28	0.15

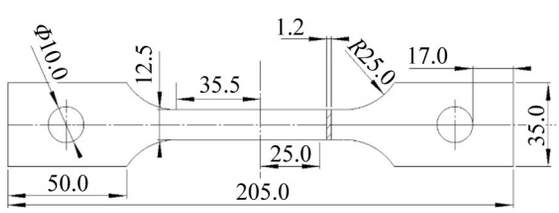

Figure 1 Two-dimensional size diagram of high temperature single tensile specimen (unit: mm)

Meanwhile, the morphology and distribution of the microstructure of original materials were preliminarily observed by an optical microscope. The test pieces need to be processed before the metallographic observation, including sampling, polishing, and then eroding with a mixed acid solution. The phase composition and distribution of the original microstructure are shown in Figure 2.

As can be seen from Figure 2, the microstructure of the sample in the polished state was a solid solution of α(Al), and more black impurity phases distributed in the matrix of α(Al). The impurity phases were evenly wrapped in a small amount of bright gray and blocky precipitated phase, the gray phase was not prone to corrosion and it may be CrAl7 primary crystal. According to the observation with high magnification, the gray clumps of the precipitated phase were wrapped in black impurity phase.

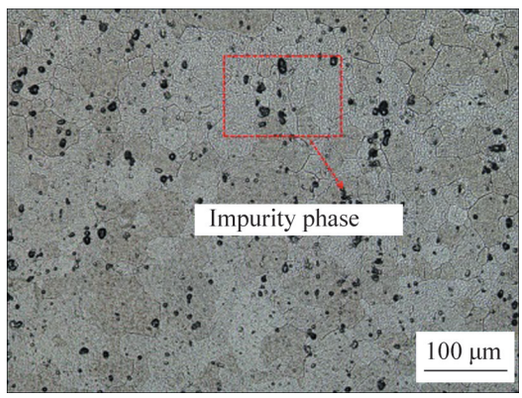

Figure 2 Original microstructure of 7075 aluminum alloy

The thermal tensile test equipment is the electronic universal testing machine E45.105. At the pre-deformation stage, the specimen is in the room temperature state, the joint area between necking and fracture is very short, and the sudden break will cause damage to the extensometer. Due to the excellent plastic flow property of the material in the high temperature environment, there is obvious transition deformation area when the necking fracture happened in the hot forming process. The artificial aging equipment is the self-developed heating furnace, and the maximum working temperature is 1200 ℃, and the control accuracy is ±1 ℃.

2.2 Experiment scheme

For the aluminum alloy parts with complex shapes and structures, because of the material properties, they can not be formed by using the traditional stamping processes, and they can not deform absolutely at once using the conventional hot forming process. Simultaneously, in order to meet the requirements of product performance and economic cost, the innovative forming technology such as indirect hot forming process was put forward. Firstly, the sheet metal was deformed at room temperature, and a certain deformation amount was obtained. Because of the dislocation movement and accumulation, the work hardening happened which makes the material obtain a certain strength. Then, the preformed part was unloaded, it was heated to the preset solid solution temperature, and it was held at this temperature for a optimized time. In this process, the crystal structure was recrystallized, the grain was refined, the plasticity of

the material was improved, and the material finished the final deformation by loading unceasingly. According to the coupling mechanism of temperature, deformation and stress in the whole hot forming, the final forming route of sheet metal can be ensured, it not only achieved the final reduction of thermal energy consumption, but also met the required strength.

Based on the scientific problems summarized from the actual production above, the indirect hot forming was developed and carried out using the unidirectional tensile tests, the test scheme is shown below: the first step is the pre-deformation process at room temperature, the specimens were stretched with two strain rates $\dot{\varepsilon}$=0.001 s^{-1}, 0.01 s^{-1} and three pre-deformation amounts ε_0=4%, 9%, 14%, respectively. The second step is sequential thermal tensile process in which the sheet metal was unloaded firstly and then heated to 480 ℃, it was kept for 10 min in this state, and then the specimens were cooled to 300 ℃, 350 ℃, 400 ℃ and 450 ℃, respectively. The tensile samples were stretched and broke at the last step.

After the compound tensile tests, the forming route can be optimized, and the optimal one can be summarized by analyzing the distribution law of the maximum tensile deformation and stress state combining the microstructure observation. The process flow diagram is shown in Figure 3.

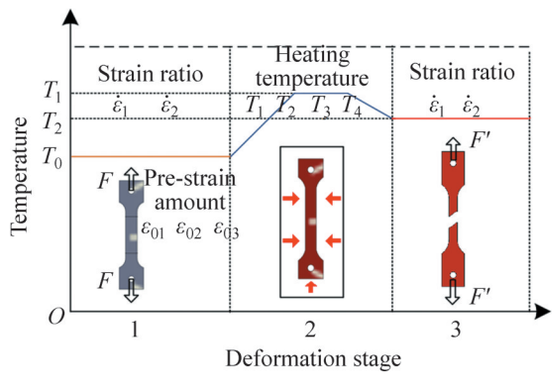

Figure 3 Compound tensile process

3 Results

3.1 Microstructure analysis

Because the compound tensile processes contain two strain rates $\dot{\varepsilon}$=0.001 s^{-1}, 0.01 s^{-1}, three pre-deformation amounts ε_0=4%, 9%, 14% and four temperatures 300 ℃, 350 ℃, 400 ℃ and 450 ℃, respectively, 24 groups of experiments have been carried out, and the broken test pieces are shown in Figures 4 and 5.

As can be seen from the tensile results shown in Figures 4 and 5, when the strain rate $\dot{\varepsilon}$=0.001 s^{-1}, there are five special test conditions: ε_0=4%, T=350/400 ℃; ε_0=9%, T=300/350 ℃; ε_0=14%, T=300 ℃, respectively, the fracture positions of the corresponding test pieces are distributed near the arc transition in all of the cases, and there will be some

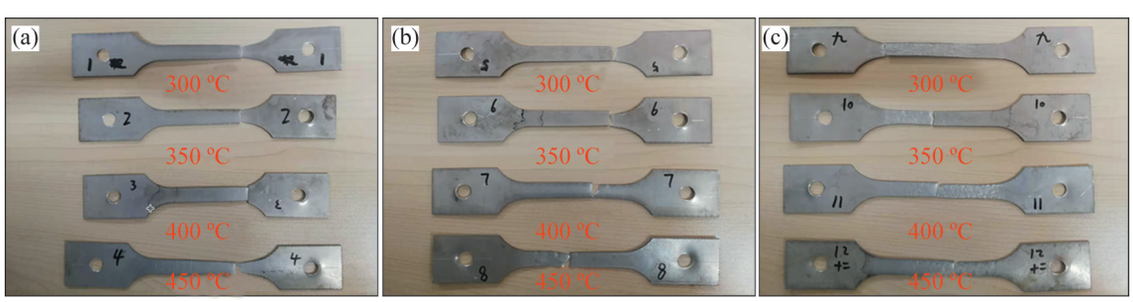

Figure 4 Broken test pieces when strain rate is 0.001 s^{-1}: (a) ε_0=4%; (b) ε_0=9%; (c) ε_0=14%

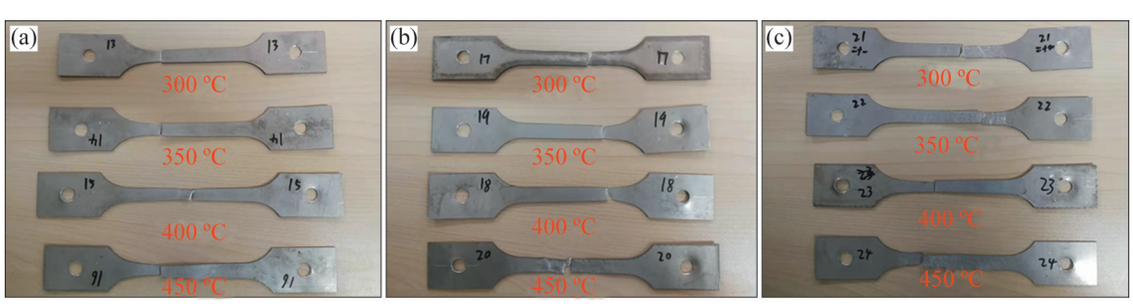

Figure 5 Broken test pieces when strain rate is 0.01 s^{-1}: (a) ε_0=4%; (b) ε_0=9%; (c) ε_0=14%

errors for the calculated elongation after fracture. The distribution regularities of elongation under all conditions are shown in Table 2.

Table 2 Elongation after fracture

Strain rate/s^{-1}	Temperature/℃	Elongation/%		
		ε_0=4%	ε_0=9%	ε_0=14%
0.001	300	38.20	31.00	48.00
	350	39.00	32.00	50.40
	400	41.00	34.68	56.88
	450	44.20	38.40	53.48
0.01	300	44.92	44.88	66.12
	350	61.72	44.48	70.12
	400	86.72	40.44	86.44
	450	63.56	37.88	62.80

Taking the forming temperature 450 ℃ for example, when the pre-deformation is ε_0=4%, 14% respectively, the elongations after fracture caused by the two kinds of strain rates are greater than the elongation after fracture caused by ε_0=9% which can be seen from Table 2. At the same time, the large strain rate causes large elongation, and the difference of the elongations for the two strain rates is 20% and 9%, respectively. It is indicated that the influence of strain rate on the forming limit is more obvious at the lower pre-deformation amount. To explain the nature of the difference between these elongations and to judge the fracture type based on microstructure distribution, the fracture morphology of specimens at 450 ℃ were analyzed using the scanning electron microscope EVO 18 from the University of Science and Technology Beijing, the accelerating voltage is 200 V − 30 kV, and the microscopic analysis results are shown in Figure 6.

As can be seen from fracture morphology, there are various dimples, it is indicated that the fracture mode of materials is ductile fracture [24 − 34], and the differences between the number and depth of the dimples morphology show the difference of the elongation. The dimples in Figures 6(d) and (f) are deep but the number is few, which indicates that the material endured severe deformation, and the deformation degree was corresponding to the maximum elongation after fracture in this state. As can be seen from Figures 6(b) and (e), the dimples are evenly distributed and are very shallow, which indicates that the degree of severe deformation is light, and the elongation after fracture is the smallest in this case.

Because the improvement of comprehensive property of AA7075 is decided by the successive solution treatment, forming, quenching and artificial aging after quenching treatment, the strengthening mechanism is as follows: the supersaturated solid solutions of aluminum alloy 7075 which are obtained by quenching treatment are in an unstable state, it has the tendency of spontaneous decomposition and exsolution, then the second strengthening phases are precipitated finally. When the aging exsolution happened, the first step is pre-exsolution period, in which solute atom segregation occurs, and the GP region forms. The second step is exsolution period, in which one or two kinds of metastable phase η' ($MgZn_2$) precipitated firstly, and the equilibrium phase η($MgZn_2$) precipitated finally [35]. So, the parameters in the solution treatment and forming process can not only affect the plasticity flow regularity and deformation limit, but also determine the comprehensive property of AA7075 ultimately. In order to verify the rationality of parameters in the solution treatment and forming process, the corresponding specimens at 450 ℃ were cooled with cooling rate of 30 ℃/s and the artificial aging treatment is 110 ℃, 4 h+150 ℃, 8 h after the thermal tensile test, and the precipitation and distribution of the corresponding second phase were observed using the metalloscope and transmission electron microscope JEM-2100F from Jilin University, as shown in Figures 7 and 8.

It can be observed from the microstructure distribution of the precipitated phase that, the precipitated phase consists of three parts: the first part is non-equilibrium binary eutectic which is formed by the α(Al), the black granular precipitated phases were T (AlZnMgCu) eutectic, and the eutectic is a kind of porous dense structure; the second part is a small number of black granule group which is the second phase precipitate η($MgZn_2$); the third part is a small amount of light gray blocky precipitated phase which is $CrAl_7$. In Figures 7(b) and (e), there are many black precipitated phases which were distributed on the grain boundary. The T (AlZnMgCu) eutectic crystals in Figures 7(d) and (f) which are in a network are more evenly distributed, and the uniform degree is

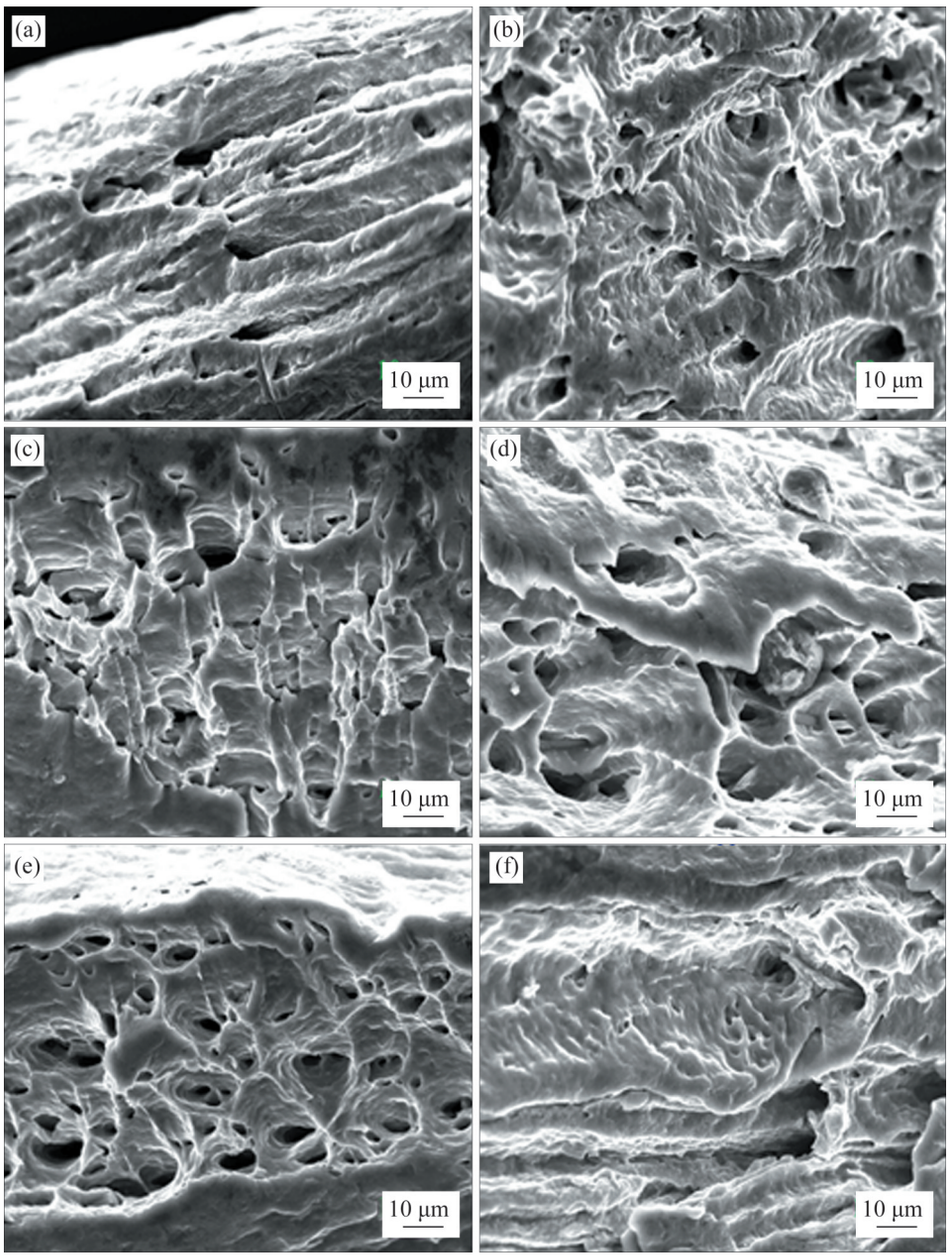

Figure 6 Distribution of the microstructure of the fracture: (a) Strain rate 0.001 s^{-1}, ε_0=4%; (b) Strain rate 0.001 s^{-1}, ε_0=9%; (c) Strain rate 0.001 s^{-1}, ε_0=14%; (d) Strain rate 0.01 s^{-1}, ε_0=4%; (e) Strain rate 0.01 s^{-1}, ε_0=9%; (f) Strain rate 0.01 s^{-1}, ε_0=14%

better than those in Figures 7(a) and (c). It is shown that the second phase precipitate η($MgZn_2$) has a tendency to hinder dislocation movement and reduce the plasticity of materials. The reticular unbalanced binary eutectic formed by T(AlZnMgCu) eutectic and matrix α(Al) can improve the movement state of grains in the deformation process due to the distribution of porous structure. In conclusion, the key process parameters such as pre-deformation and strain rate in indirect hot forming of 7075 aluminum alloy will also affect the distribution of second phase after artificial aging, and the strength of the aluminum alloy was eventually improved. Therefore, the suitable combination of pre-deformation, strain rate, and forming temperature can not only improve the forming property but also play an important role in the strength improvement of the product after forming.

As can be seen from Figure 8, the precipitated phases are mainly rod-shaped, a small number of precipitated phases are ellipsoid-shaped, and they

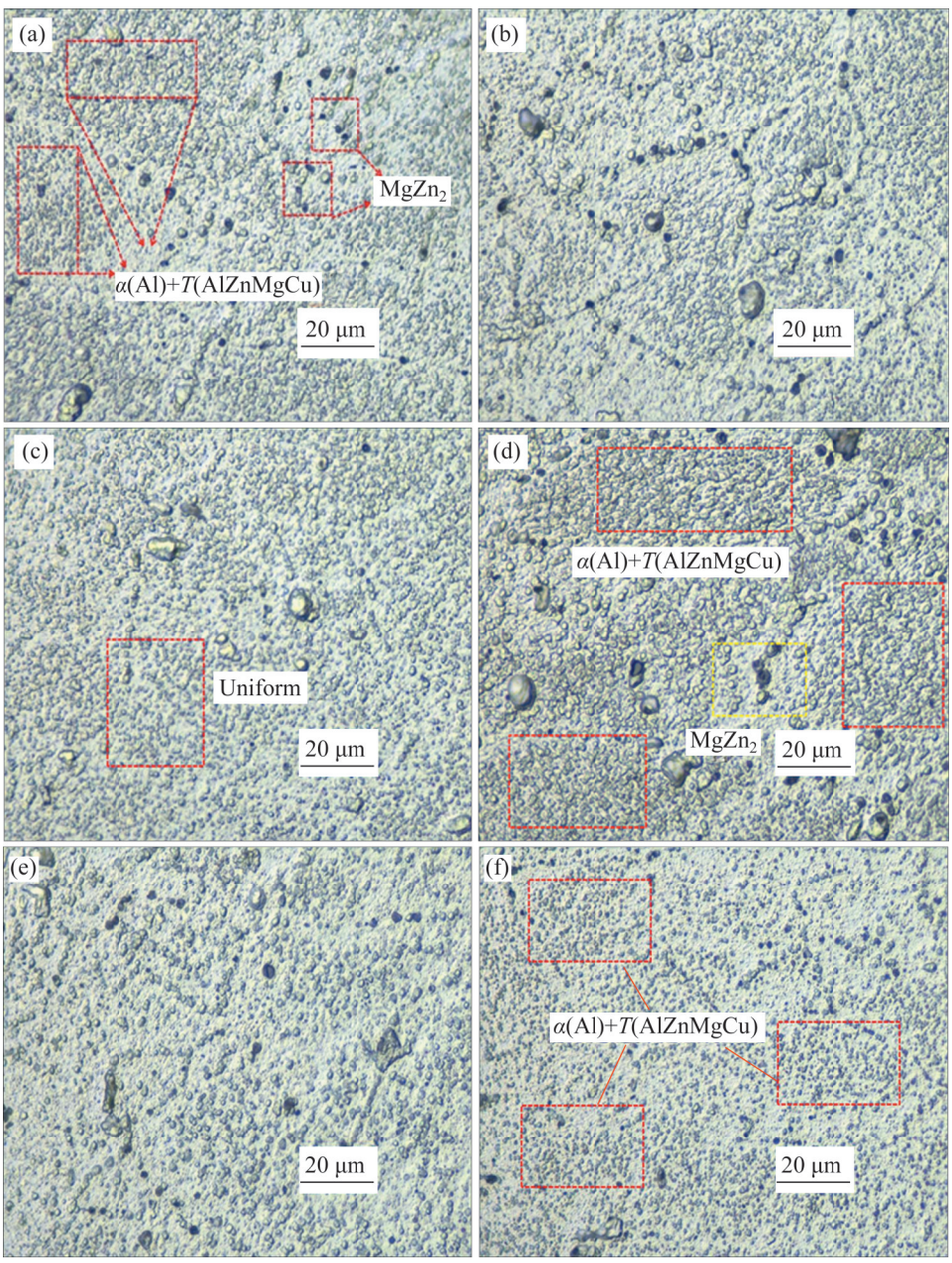

Figure 7 Distribution of the second precipitated phase: (a) Strain rate 0.001 s^{-1}, ε_0=4%; (b) Strain rate 0.001 s^{-1}, ε_0=9%; (c) Strain rate 0.001 s^{-1}, ε_0=14%; (d) Strain rate 0.01 s^{-1}, ε_0=4%; (e) Strain rate 0.01 s^{-1}, ε_0= 9%; (f) Strain rate 0.01 s^{-1}, ε_0=14%

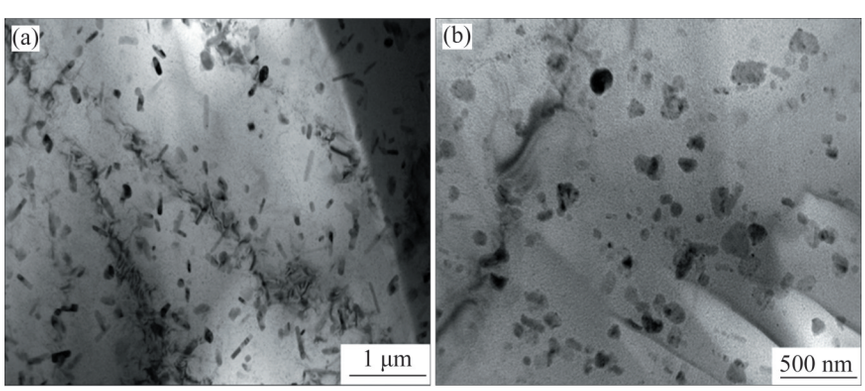

Figure 8 Precipitation distribution after the artificial aging treatment of 110 ℃, 4 h+150 ℃, 8 h

are all distributed uniformly. Among them, there are a large number of small precipitated phases which are in the grain, and a small number of precipitated phases are distributed on the crystal boundary. Inside the grain, the farther away from the crystal boundary, the more the precipitated phases. The precipitated phases at the crystal boundary play a role in strengthening the crystal boundary. When the dislocation occurred in the grain, a large number of precipitate phases around the dislocation will hinder the movement of the dislocation, playing a pinning role, and effectively improve the performance finally.

In conclusion, it can be seen from the quantitative analyses of fracture morphology distribution and elongation after fracture that, the material has an obvious strain rate sensitivity to the pre-deformation degree (ε_0=4%, 14%). In the intermediate state (ε_0=9%), the strain rate sensitivity is not obvious. Therefore, the indirect hot forming processes in which the pre-deformation amount is 4% and 14% respectively are useful for the formation of parts with relatively large deformation amounts. According to the analysis of production capacity at present, the appropriate deformation rate can be selected simultaneously to achieve the ultimate purpose of large deformation.

The elongation after break is an important parameter to characterize the ductility in the deformation process. The better the extensibility, the easier the material is to bear the force and the greater the safety stock. In this paper, the distributions of elongation after different pre-deformation, strain rates, and forming temperatures were studied. At the same time, the influence of different combinations of indirect hot forming process parameters on the ductility of material was revealed.

3.2 Deformation analysis

After the complex tensile process, the deformations of the specimens at different group cases were analyzed. According to the data collation, the displacement−stress curves were obtained, as shown in Figure 9, and Δ_1, Δ_2, Δ_3 represent the difference between the maximum deformation amount in the case of adjacent temperature respectively.

As can be seen from Figure 9 that, when the pre-deformation at room temperature was complete, the sample was unloaded and then loaded again in the thermal environment sequentially, the sample was deformed and rapidly reached the tensile limit state. At the same time, when the strain rate and the pre-deformation amount kept invariable, there is a significant difference between those specimens at different forming temperatures, which indicates the material has obvious temperature sensitivity. In the hot forming stage, the tensile strength of the material was significantly lower than that at room temperature, because dynamic recrystallization and grain refinement happened in the thermal environment, and obvious softening effect of the material was observed. According to the analysis of the displacement−stress curves, it is illustrated that when the strain rate is 0.001 s^{-1} and 0.01 s^{-1} respectively, there is no linear relationship among the pre-deformation, forming temperature, and the tensile strength limit, and there is no certain regularity.

As can be seen from the above deformation data, it is known that the deformation law of material is comprehensively affected by the three process parameters $f=f(\varepsilon_0, \dot{\varepsilon}, T)$ in the indirect forming process. When the strain rate is 0.001 s^{-1}, with the increase of the pre-deformation degree, the lower the temperature is, the greater the final deformation is. When the strain rate is $\dot{\varepsilon}$=0.01s^{-1}, with the increase of the pre-deformation degree, the higher the temperature is, the greater the final deformation is.

At the same time, under the condition of the same pre-deformation, the larger the strain rate is, the larger the deformation is. It is illustrated that the comprehensive effect of work hardening in the pre-deformation stage, work hardening in the hot forming stage and softening mechanism of fine grain on the plastic flow law of the material is complex.

All of these can be summed up that when strain rate is 0.001 s^{-1}, the pre-deformation is ε_0=4% and the temperature is 450 °C, respectively, the maximum deformation amount is 26 mm. When the pre-deformation is ε_0=9%, the temperature is 400 °C, the maximum deformation amount is about 18 mm. When the pre-deformation is 14%, the maximum deformation amount is about 27 mm at 300 °C; When the strain rate is 0.01 s^{-1}, the pre-

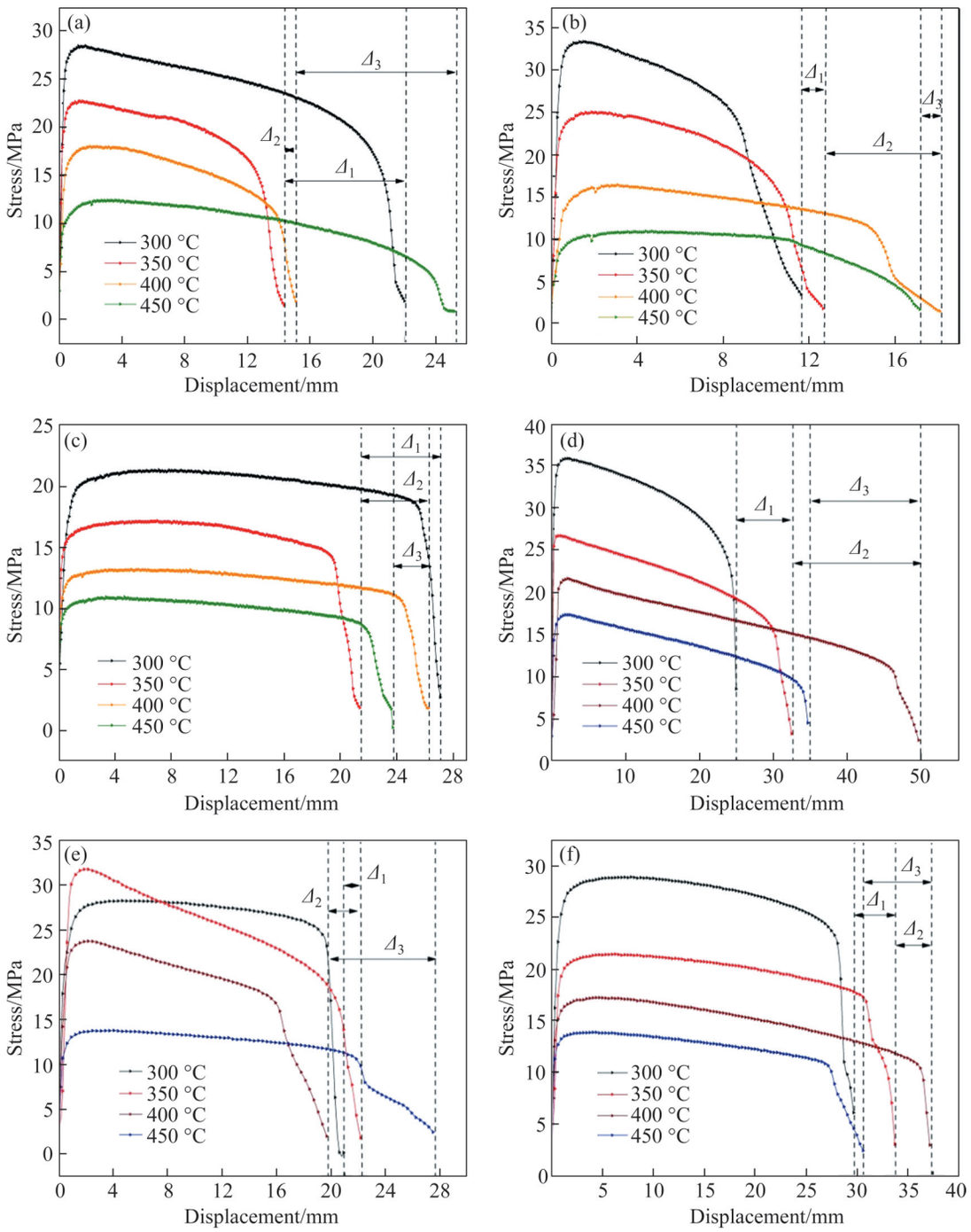

Figure 9 Distribution of displacement−stress curves: (a) Strain rate 0.001 s^{-1}, ε_0=4%; (b) Strain rate 0.001 s^{-1}, ε_0= 9%; (c) Strain rate 0.001 s^{-1}, ε_0=14%; (d) Strain rate 0.01 s^{-1}, ε_0= 4%; (e) Strain rate 0.01 s^{-1}, ε_0= 9%; (f) Strain rate 0.01 s^{-1}, ε_0= 14%

deformation is ε_0=4%, the maximum deformation amount reaches 50 mm at 400 ℃. When the pre-deformation is ε_0=9%, the maximum deformation amount reaches about 28 mm at 450 ℃. When the pre-deformation is ε_0=14%, the maximum deformation amount reaches about 37.5 mm at 400 ℃.

Based on the deformation analysis above, the technology route can be summarized from the viewpoint of maximum deformation amount: when the strain rate is $\dot{\varepsilon}$=0.001 s^{-1}, the optimum forming temperature is chosen as 450 ℃, 400 ℃, 300 ℃, respectively. While, when the strain rate is 0.01 s^{-1}, with the increase of the pre-deformation, the

optimum forming temperature is 400 ℃, 450 ℃, 400 ℃, respectively.

3.3 Stress analysis

After the test, the influence of the multi-field coupling process on the peak stress was quantitatively analyzed, and the distribution of stress was analyzed by combining the deformation mechanisms such as work hardening effect and hot softening effect. At the same time, the peak stresses with different pre-deformation degree were drawn, which are shown in Figure 10.

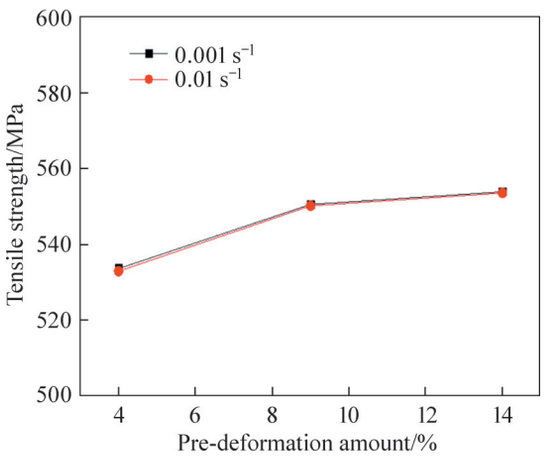

Figure 10 Distribution of tensile stress with different pre-deformation at room temperature

It can be seen from the distribution trends of tensile strength shown in Figure 10, when the strain rate changed, the peak stress is very close at the same pre-deformation, and it is illustrated that the material is not sensitive to the deformation rate at room temperature. The distribution regularities of the peak stress during the compound tensile process are shown in Table 3.

As shown in Table 3, the work hardening mechanism makes the deformation resistance increase after the deformation with different strain rates and a certain amount of pre-deformation. While, because of unstable deformation energy in the grain boundary, it can absorb heat activation energy in the thermal environment and then transform to a stable state. The reactivation of accumulated dislocation and grain refinement make the plasticity improve, which demonstrated macroscopically that a small driving force can perform the same plastic deformation. When the strain rate $\dot{\varepsilon}$=0.001 s^{-1}, the pre-deformation is 9%, the corresponding tensile strength changed suddenly, and the value is the largest when the forming temperature is 300 ℃. However, when the strain rate is $\dot{\varepsilon}$=0.01 s^{-1}, the pre-deformation is 9%, the corresponding tensile strength changed suddenly too, but the value is the largest when the forming temperature is 350 ℃. It was concluded that the pre-deformation is the main factor affecting the deformation resistance of the compound tensile process.

Table 3 Peak strengths of specimens during the compound tensile process

Strain rate/s^{-1}	Temperature/℃	Peak strength/MPa		
		ε_0=4%	ε_0=9%	ε_0=14%
0.001	300	28.45	33.47	21.37
	350	22.75	25.09	17.21
	400	18.06	16.49	13.27
	450	12.47	11.0	10.97
0.01	300	35.83	28.25	28.93
	350	26.74	31.76	21.45
	400	21.65	23.75	17.27
	450	17.38	13.79	13.91

As can be seen from Table 3, when the strain rate is 0.001 s^{-1} and the forming temperature changes in the range of 300 − 350 ℃, with the increase of the deformation temperature, the tensile strength at the pre-deformation ε_0=9% is the maximum; When the forming temperature changes in the range of 350 − 450 ℃, the tensile strength at the pre-deformation ε_0=4% is the maximum. When the strain rate is 0.01 s^{-1}, and the forming temperature is 300 ℃ and 450 ℃, respectively, the tensile strength of the material with the pre-deformation ε_0=4% is the maximum; When the forming temperature changes in the range of 350 − 400 ℃, the tensile strength of the material with the pre-deformation ε_0=9% is the maximum. Among all the deformation conditions, when the pre-deformation is ε_0=14%, the tensile strength of the material was the weakest.

In the process of compound forming, it is indicated that the stress state of the material is significantly affected by strain rate, deformation temperature, and low pre-deformation (ε_0=4%, 9%), and it is not sensitive to large pre-deformation obviously.

4 Conclusions

According to a series of unidirectional tensile tests of the indirect hot forming technology, it is illustrated that the plasticity property of the material at the forming process was affected by many parameters such as pre-deformation, strain rate and forming temperature. The microstructure after heat treatment was affected by the comprehensive effect of these parameters at the same time, so the strength of the material is significantly different. By studying the plasticity deformation behavior of AA7075 considering the pre-deformation (work hardening), strain rate, and temperature, the followings were concluded:

1) It is known from the stress − displacement curves of the material after the indirect forming process, the plastic rheological behavior of the material is sensitive to the pre-deformation, strain rate, and forming temperature. Moreover, when the strain rate is $\dot{\varepsilon}$=0.01 s^{-1}, the pre-deformation amount is 4% and the forming temperature is 400 ℃, the deformation amount of the material is maximum and the value is 50 mm.

2) It can be seen from the distribution of peak stress that the peak stress is significantly sensitive to strain rate, forming temperature, and low pre-deformation (ε_0=4%, 9%). When the strain rate is $\dot{\varepsilon}$=0.001 s^{-1} and the pre-deformation amount is 4% and 9% respectively, the peak stress of the material is 533.45 MPa and 533.47 MPa, respectively. When the strain rate is 0.01 s^{-1} and the pre-deformation amount is 4% and 9%, respectively, the peak stress of the material is 550.85 MPa and 550.76 MPa, respectively.

3) Combining with the elongation after fracture and the fracture morphology, the plasticity flow behavior of the material in the hot forming process was plastic and it was judged to be related to the pre-deformation, strain rate, and forming temperature, and it is demonstrated that the distribution of the elongation after fracture is regular in the complex forming process. According to the analysis of deformation amount and stress distribution, it contributes to the optimal route establishment of the indirect hot forming of aluminum alloy, and it is of great significance for the popularization and application of the lightweight technology.

Contributors

The overarching research goals were developed by ZHANG Quan-da, SUN Fu-zhen, LIU Meng, and LIU Wen-cai. ZHANG Quan-da provided the concept and edited the draft of manuscript. SUN Fu-zhen and LIU Meng carried out the tensile tests and analyzed the measured data. LIU Wen-cai performed metallographic test and TEM test, and observed the microstructure and precipitated phase. All authors replied to reviewers' comments and revised the final version.

Conflict of interest

ZHANG Quan-da, SUN Fu-zhen, LIU Meng, and LIU Wen-cai declare that they have no conflict of interest.

References

[1] HIRSCH J, AL-SAMMAN T. Superior light metals by texture engineering: Optimized aluminum and magnesium alloys for automotive applications [J]. Acta Materialia, 2013, 61(3): 818−843. DOI: 10.1016/j.actamat.2012.10.044.

[2] SHE Huan, SHU Da, DONG An-ping, et al. Relationship of particle stimulated nucleation, recrystallization and mechanical properties responding to Fe and Si contents in hot-extruded 7055 aluminum alloys [J]. Journal of Materials Science & Technology, 2019, 35(11): 2570 − 2581. DOI: 10.1016/j.jmst.2019.07.014.

[3] YANG Yong-biao, ZHANG Zhi-min, LI Xu-bin, et al. The effects of grain size on the hot deformation and processing map for 7075 aluminum alloy [J]. Materials & Design, 2013, 51: 592−597. DOI: 10.1016/j.matdes.2013.04.034.

[4] FAN Xi-gang, JIANG Da-ming, MENG Qing-chang, et al. The microstructural evolution of an Al-Zn-Mg-Cu alloy during homogenization [J]. Materials Letters, 2006, 60(12): 1475−1479. DOI: 10.1016/j.matlet.2005.11.049.

[5] LIU Xiao-yan, PAN Qing-lin, FAN Xi, et al. Microstructural evolution of Al-Cu-Mg-Ag alloy during homogenization [J]. Journal of Alloys and Compounds, 2009, 484(1 − 2): 790 − 794. DOI: 10.1016/j.jallcom.2009.05.046.

[6] CHEGINI M, SHAERI M H. Effect of equal channel angular pressing on the mechanical and tribological behavior of Al-Zn-Mg-Cu alloy [J]. Materials Characterization, 2018, 140: 147−161. DOI: 10.1016/j.matchar.2018.03.045.

[7] ZHANG Xian-feng, LU Zheng, GAO Wen-li, et al. Heat treatment process of 7AXX aluminum alloy [J]. Heat Treatment of Metals, 2012, 37(2): 65−69. DOI: CNKI:SUN: JSRC.0.2012-02-015.

[8] ZAEFFERER S, KUO J C, ZHAO Z, et al. On the influence of the grain boundary misorientation on the plastic deformation of aluminum bicrystals [J]. Acta Materialia, 2003, 51(16): 4719 − 4735. DOI: 10.1016/S1359-6454(03) 00259-3.

[9] MERRIMAN C C, FIELD D P, TRIVEDI P. Orientation dependence of dislocation structure evolution during cold rolling of aluminum [J]. Materials Science and Engineering A, 2008, 494(1 − 2): 28 − 35. DOI: 10.1016/j.msea.2007.10.090.

[10] XIAO Guan-fei, JIANG Ju-fu, LIU Ying-ze, et al. Recrystallization and microstructure evolution of hot extruded 7075 aluminum alloy during semi-solid isothermal treatment [J]. Materials Characterization, 2019, 156: 109874. DOI: 10.1016/j.matchar.2019.109874.

[11] ROKNI M R, ZAREI-HANZAKI A, ABEDI H R. Microstructure evolution and mechanical properties of back extruded 7075 aluminum alloy at elevated temperatures [J]. Materials Science and Engineering A, 2012, 532: 593 − 600. DOI: 10.1016/j.msea.2011.11.020.

[12] ABEDRABBO N, POURBOGHRAT F, CARSLEY J. Forming of aluminum alloys at elevated temperatures-Part 1: Material characterization [J]. International Journal of Plasticity, 2006, 22(2): 314 − 341. DOI: 10.1016/j. ijplas. 2005.03.005.

[13] XIAO Wen-chao. Study of unified viscoplastic constitutive modeling and key technologies of hot stamping of 7075 aluminum sheet [D]. Beijing: University of Science and Technology Beijing, 2018. (in Chinese)

[14] OMER K, ABOLHASANI A, KIM S, et al. Process parameters for hot stamping of AA7075 and D-7xxx to achieve high performance aged products [J]. Journal of Materials Processing Technology, 2018, 257: 170−179. DOI: 10.1016/j.jmatprotec.2018.02.039.

[15] BARIANI P F, BRUSCHI S, GHIOTTI A, et al. Hot stamping of AA5083 aluminum alloy sheets [J]. CIRP Annals Manufacturing Technology, 2013, 62(1): 251 − 254. DOI: 10.1016/j.cirp.2013.03.050.

[16] XIAO Wen-chao, WANG Bao-yu, ZHENG Kai-lun. An experimental and numerical investigation on the formability of AA7075 sheet in hot stamping condition [J]. The International Journal of Advanced Manufacturing Technology, 2017, 92(9 − 12): 3299 − 3309. DOI: 10.1007/s00170-017-0419-6.

[17] ROKNI M R, ZAREI-HANZAKI A, ROOSTAEI A A, et al. An investigation into the hot deformation characteristics of 7075 aluminum alloy [J]. Materials & Design, 2011, 32(4): 2339−2344. DOI: 10.1016/j.matdes.2010.12.047.

[18] MA Ka-ka, WEN Hai-ming, HU Tao, et al. Mechanical behavior and strengthening mechanisms in ultrafine grain precipitation-strengthened aluminum alloy [J]. Acta Materialia, 2014, 62: 141−155. DOI: 10.1016/j.actamat.2013.09.042.

[19] MA Ka-ka, HU Tao, YANG H, et al. Coupling of dislocations and precipitates: Impact on the mechanical behavior of ultrafine grained Al-Zn-Mg alloys [J]. Acta Materialia, 2016, 103: 153−164. DOI: 10.1016/j.actamat.2015.09.017.

[20] WERT J A, PATON N E, HAMILTON C H, et al. Grain refinement in 7075 aluminum by thermomechanical processing [J]. Metallurgical Transactions A, 1981, 12(7): 1267−1276. DOI: 10.1007/BF02642340.

[21] MOHAMED M S, FOSTER A D, LIN Jian-guo, et al. Investigation of deformation and failure features in hot stamping of AA6082: Experimentation and modelling [J]. International Journal of Machine Tools and Manufacture, 2012, 53(1): 27−38. DOI: 10.1016/j.ijmachtools.2011.07.005.

[22] EL-MAGD E, ABOURIDOUANE M. Characterization, modelling and simulation of deformation and fracture behaviour of the light-weight wrought alloys under high strain rate loading [J]. International Journal of Impact Engineering, 2006, 32(5): 741 − 758. DOI: 10.1016/j.ijimpeng.2005.03.008.

[23] LI X C. Microstructure and metallographic atlasof aluminum alloy [M]. Beijing: Metallurgical Industry Press, 2010. ISBN: 978-7-5024-5263-6. (in Chinese)

[24] SONG Z. Flow stress characteristics and constitutive equation at high temperature for 7050 aluminum alloy [J]. Journal of Wuhan University of Technology, 2006, 28: 113−116. DOI: 10.1016/S1872-1508(06)60066-1.

[25] FU X, AI X, LIU Z, WAN Y. Study on shear angle model of aluminum alloy 7050-T7451 in high speed machining [J]. China Mechanical Engineering, 2007, 18: 220 − 224. (in Chinese)

[26] HU H E, ZHEN L, YANG L, et al. Deformation behavior and microstructure evolution of 7050 aluminum alloy during high temperature deformation [J]. Materials Science and Engineering A, 2008, 488(1 − 2): 64 − 71. DOI: 10.1016/j.msea.2007.10.051.

[27] GAO Yu-hua. Dynamic compression and tensile properties of Al alloys LC4 and LY12CZ at high strain rate [J]. Material Science and Technology, 1994, 2(2): 24−29.

[28] PENG Kai-ping, CHEN Wen-zhe, QIAN Kuang-wu. Study on dynamic strain aging phenomenon of 3004 aluminum alloy [J]. Materials Science and Engineering A, 2006, 415(1−2): 53−58. DOI: 10.1016/j.msea.2005.08.216.

[29] LEE W S, SUE W C, LIN Chi-feng, et al. The strain rate and temperature dependence of the dynamic impact properties of 7075 aluminum alloy [J]. Journal of Materials Processing Technology, 2000, 100(1−3): 116−122. DOI: 10.1016/S0924-0136(99)00465-3.

[30] YANG H T, LU Z, GU J L. Study on the flow stress of 7A60 ultra high strength aluminum alloy [J]. Journal of Aeronautical Materials, 2005, 2: 12 − 15. DOI: 10.3969/j.issn.1005-5053.2005.02.003.

[31] YANG Yong, KE Ying-lin, DONG Hui-yue. Study on correlation between parameters of “single factor” constitutive model and temperature for 7050 aviation aluminum-alloy [J]. Journal of Aeronautical Materials, 2007, 27 (4): 19−24. (in Chinese)

[32] YANG Yong, KE Ying-lin, DONG Hui-yue. Constitutive model of aviation aluminum-alloy material in metal machining [J]. The Chinese Journal of Nonferrous Metals, 2005(6): 854−859. (in Chinese)

[33] PEDERSEN K O, WESTERMANN I, FURU T, et al. Influence of microstructure on work-hardening and ductile fracture of aluminium alloys [J]. Materials & Design, 2015, 70: 31−44. DOI: 10.1016/j.matdes.2014.12.035.

[34] THAM Y W, FU M W, HNG H H, et al. Bulk nanostructured processing of aluminum alloy [J]. Journal of Materials Processing Technology, 2007, 192 − 193: 575 − 581. DOI: 10.1016/j.jmatprotec.2007.04.076.

[35] PAGLIA C S, JATA K V, BUCHHEIT R G. The influence of artificial aging on the microstructure, mechanical properties, corrosion, and environmental cracking susceptibility of a 7075 friction-stir-weld [J]. Materials and Corrosion, 2007, 58(10): 737−750. DOI: 10.1002/maco.200704063.

(Edited by HE Yun-bin)

中文导读

利用间接热成形技术优化热处理Al-Zn-Mg-Cu合金的微观组织和力学性能

摘要：本文开展了7075铝合金的间接热拉伸试验和材料塑性变形行为研究，同时包含间接热成形和热处理技术。试验过程考虑了3种预变形量，2种应变速率和4种成形温度。在间接热成形过程中，材料对预变形，应变速率和成形温度是敏感的。当应变速率为$\dot{\varepsilon}$=0.01 s^{-1}，预变形量为ε_0=4%，成形温度为T=400 ℃时，材料的最大拉伸变形量为50 mm。以成形温度为450 ℃的情况为例，通过断口微观形貌的观察，材料在热成形过程的断裂形式为塑性断裂。通过观察经过淬火和时效处理后的试样微观组织可知，T(AlZnMgCu)共晶体与基体α(Al)形成了网状的非平衡二元共晶体。

关键词：应变速率；预变形；成形温度；7075铝合金；复合拉伸